

Project Report
LSP-355

Wide-Field-of-View Lyot Filter: FY21 Line-Supported Optical Systems Program

M.J. Polking
W.D. Herzog
S. Kaushik
S.M. Redmond
K.J. Tibbets
C.A. Primmerman

03 May 2022

Lincoln Laboratory
MASSACHUSETTS INSTITUTE OF TECHNOLOGY
LEXINGTON, MASSACHUSETTS



DISTRIBUTION STATEMENT A. Approved for public release. Distribution is unlimited.

This material is based upon work supported by the Under Secretary of Defense for Research and Engineering under Air Force Contract No. FA8702-15-D-0001.

This report is the result of studies performed at Lincoln Laboratory, a federally funded research and development center operated by Massachusetts Institute of Technology. This material is based upon work supported by the Under Secretary of Defense for Research and Engineering under Air Force Contract No. FA8702-15-D-0001. Any opinions, findings, conclusions or recommendations expressed in this material are those of the author(s) and do not necessarily reflect the views of the Under Secretary of Defense for Research and Engineering.

© 2022 Massachusetts Institute of Technology

Delivered to the U.S. Government with Unlimited Rights, as defined in DFARS Part 252.227-7013 or 7014 (Feb 2014). Notwithstanding any copyright notice, U.S. Government rights in this work are defined by DFARS 252.227-7013 or DFARS 252.227-7014 as detailed above. Use of this work other than as specifically authorized by the U.S. Government may violate any copyrights that exist in this work.

Massachusetts Institute of Technology
Lincoln Laboratory

Wide-Field-of-View Lyot Filter: FY21 Line-Supported
Optical Systems Program

M.J. Polking

K.J. Tibbetts

W.D. Herzog

Group 81

S. Kaushik

Group 91

C.A. Primmerman

Division 9

Project Report LSP-355

03 May 2022

DISTRIBUTION STATEMENT A. Approved for public release. Distribution is unlimited.

This material is based upon work supported by the Under Secretary of Defense for Research and Engineering under Air Force Contract No. FA8702-15-D-0001. Any opinions, findings, conclusions or recommendations expressed in this material are those of the author(s) and do not necessarily reflect the views of the Under Secretary of Defense for Research and Engineering.

Lexington

Massachusetts

ABSTRACT

Lyot filters employ differential phase retardation for orthogonal polarizations of light induced by stacks of birefringent waveplates. Lyot filters are widely used for filtering the emission spectra of tunable lasers and for astronomical imaging, particularly for solar observation. Achieving filters with simultaneously high spectral resolution, free spectral range, and field of view, however, remains an outstanding challenge. In this paper, a novel concept for a Lyot filter is described that employs a combination of two materials with opposing signs for both birefringence magnitude and dispersion. An analytical model of this design indicates that a large field of view can be achieved while maintaining high spectral resolution and free spectral range for material combinations that yield a zero-crossing of the birefringence magnitude but a large birefringence dispersion. Candidate material combinations for the novel filter design are surveyed, first with experimental data for common birefringent materials, and subsequently with automated database mining algorithms and first-principles materials theory. The top candidate material pairs are then screened for projected impact on filter performance using the analytical filter design model. Broad screening of candidate materials indicates that the material pair of HgI and GaSe yields a birefringence dispersion of $7 \times 10^{-4} \text{ nm}^{-1}$, sufficient to enable a spectral resolution of 0.05 nm for a practically achievable maximum plate thickness of 1 cm. Approaches for synthesis of single-crystal specimens of top candidate materials are then surveyed, and an apparatus for flux crystallization of candidate materials is described.

This page intentionally left blank.

TABLE OF CONTENTS

	Page
ABSTRACT	iii
List of Illustrations	vii
List of Tables	ix
INTRODUCTION	1
1. OPTICAL MODEL OF LYOT FILTER	5
2. STRATEGY FOR MEETING MATERIAL PROPERTY REQUIREMENTS	11
3. INITIAL SCREENING OF CANDIDATE MATERIALS	13
4. BROADER SCREENING OF CANDIDATE MATERIALS	19
5. COMPUTATIONAL SCREENING OF CANDIDATE MATERIALS	23
6. EVALUTION OF CANDIDATE MATERIALS FOR LYOT FILTER	25
7. SELECTION OF MATERIALS FOR EXPERIMENTAL SYNTHESIS	29
8. DESIGN AND CONSTRUCTION OF CRYSTAL GROWTH APPARATUS	31
SUMMARY AND CONCLUSIONS	33
References	35

This page intentionally left blank.

LIST OF ILLUSTRATIONS

Figure No.		Page
1	Design and output of a conventional Lyot filter. A conventional 4-stage Lyot filter (left) and the spectral output of each stack and the final filter output (right).	2
2	Comparison of conventional Lyot-filter stack with novel Lyot-filter stack using two materials.	3
3	Birefringent plate thickness required for the “thin” stage of a Lyot filter vs. birefringence dispersion for various spectral bandwidths. Zero birefringence at a center operating wavelength of 1000 nm is assumed.	7
4	Birefringent plate thickness required for the thickest stage of a Lyot filter vs. birefringence dispersion for various spectral resolutions. Zero birefringence at a center operating wavelength of 1000 nm is assumed.	8
5	Refractive indices (A) and birefringence (B) for GaN based on Density Functional Theory calculations. GaN exhibits “anomalous” birefringence dispersion, meaning the magnitude of the birefringence increases as a function of wavelength.	11
6	Pathway to achieving simultaneously a zero crossing in the birefringence and a large birefringence dispersion.	12
7	Birefringence dispersion of a LiNbO ₃ /GaN composite. For the calculated dispersion level, a maximum stage thickness of >0.5 m would be required to achieve even a modest 1 nm spectral resolution.	13
8	Analysis of the birefringence and birefringence dispersion for a composite of TiO ₂ and GaSe. A. Optical constants for TiO ₂ and GaSe; B. Birefringence vs. wavelength for TiO ₂ and GaSe; C. Composite birefringence vs. wavelength for combinations of TiO ₂ and GaSe ranging from pure TiO ₂ to pure GaSe; D. Birefringence dispersion for an optimized composite with a zero crossing.	16
9	Birefringence dispersion of an optimized TiO ₂ /GaSe composite. A large improvement can be seen compared to the originally proposed GaN/ LiNbO ₃ composite, but the maximum stage thickness remains prohibitive.	17
10	Materials Project entry for GaN showing structure, stability, and bandgap data.	19

LIST OF ILLUSTRATIONS (Continued)

Figure No.		Page
11	Dielectric properties for GaN from the Materials Project database.	20
12	Optical properties for HgBr calculated with Density Functional Theory, including refractive indices (A), extinction coefficients (B), birefringence (C), and birefringence dispersion (D).	24
13	Analysis of the birefringence and birefringence dispersion for a composite of HgI and GaSe. A. Optical constants for HgI and GaSe; B. Birefringence vs. wavelength for HgI and GaSe; C. Composite birefringence vs. wavelength for combinations of HgI and GaSe ranging from pure HgI to pure GaSe; D. Birefringence dispersion for an optimized composite with a zero crossing.	25
14	Birefringence dispersion of optimized HgI/GaSe composite. A large improvement can be seen compared to the originally proposed GaN/ LiNbO ₃ composite, and reasonable filter performance parameters can be achieved for experimentally feasible maximum stage thickness values.	26
15	Comparison of experimental (left) and calculated (right) optical constants for GaSe. Anomalous birefringence dispersion can be observed in both theory and experiment over the range of 0.6–0.9 microns.	28
16	Apparatus for growth of single crystals using precipitation from solution. Crystals can be grown either by slow, controlled evaporation of solvent or by slow cooling of a saturated solution.	31

LIST OF TABLES

Table No.		Page
1	Specifications for Optical Filter	1
2	Survey of common birefringent materials. The originally proposed materials, LiNbO ₃ and GaN, are highlighted in yellow, and the optimum combination of materials from among those surveyed is highlighted in green.	14
3	Top 20 candidate materials extracted from the Materials Project database ranked by anisotropy in the high-frequency dielectric tensor. Candidate materials have a bandgap greater than 2 eV and are within 10 meV/atom of the convex hull.	21
4	Comparison of materials with anomalous birefringence dispersion. Anomalous dispersion appears to be common for particular material families, defined by generic chemical formula and space group.	27
5	Comparison and prioritization of top candidate materials for experimental validation.	29

This page intentionally left blank.

INTRODUCTION

The objective of this project is to explore a novel concept for a tunable, wideband, wide-field-of-view (WFOV) optical filter. Specifications for this filter are given in Table 1. These specifications are quite stringent. In particular, we highlight that the filter must have extremely narrow resolution (0.05 nm), but pass > 50% of the light in this band. It must be tunable over a wavelength range that goes from short-wavelength visible to 1600 nm in the near infrared (NIR).

TABLE 1
Specifications for Optical Filter

Performance Parameters	Target Values
Wavelength range	500–1600 nm
Spectral resolution	0.05 nm
Peak optical transmission	> 50%
Aperture	~ 1 cm
Angular FOV	+/-30°
Length	<10 cm
Wavelength-tunable	Yes
Out-of-band suppression	>20 dB

The filter being developed is an extension of a conventional Lyot filter [1], one implementation of which is shown in Figure 1. A conventional Lyot filter comprises multiple stacks of filter elements, where each stack has a birefringent waveplate and a polarizer. The transmission of each stack is approximately sinusoidal as a function of wavelength, as shown in Figure 1. The thicknesses of the birefringent waveplates vary by factors of two. The full Lyot filter can have a very narrowband output, as shown in Figure 1. The resolution is given by the thickest birefringent crystal; the free spectral range is given by the thinnest birefringent crystal.

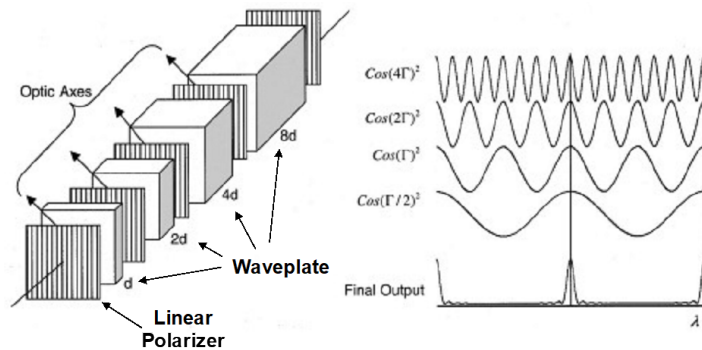


Figure 1. Design and output of a conventional Lyot filter. A conventional 4-stage Lyot filter (left) and the spectral output of each stack and the final filter output (right) [2].

Conventional Lyot filters are widely used in astronomy and, in fact, have spaceflight heritage [3]. Their principal drawback is that there is no known method to make them broadly tunable from the visible through the NIR.

The waveplate in a conventional Lyot filter uses a uniaxial crystal with zero-crossing birefringence (e.g., quartz). To extend the Lyot-filter performance, one of the authors (S. Kaushik) came up with the novel concept to make the waveplate out of two materials—one positive uniaxial and the other negative uniaxial. The novel concept is schematically illustrated in Figure 2. The zero-birefringence crossing is, thus, achieved using materials with different dispersion and birefringence. Using two materials instead of one means that the filter does not need to operate near an absorption edge and should, in principle, enable WFOV performance from the visible through the NIR. Achieving the specified performance in practice, however, requires finding two complementary materials with appropriate optical properties.

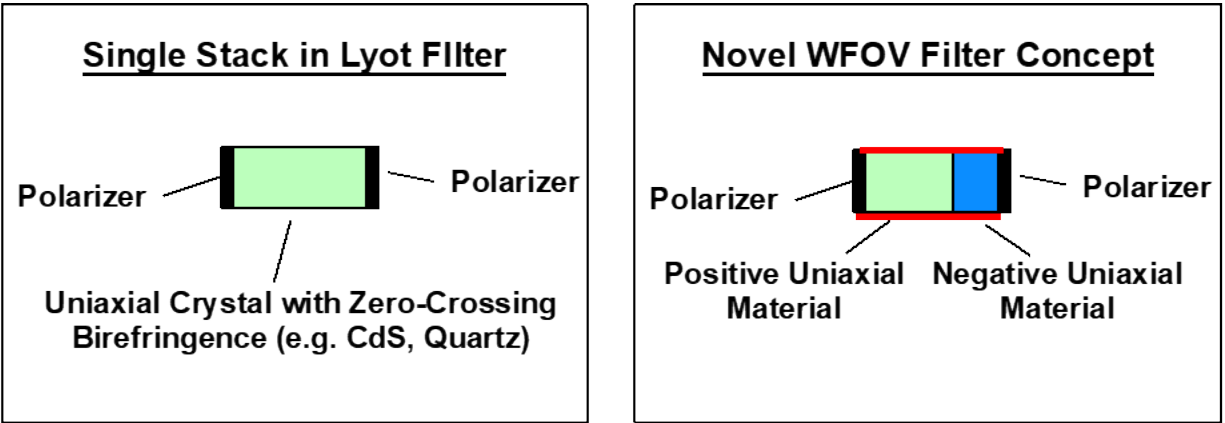


Figure 2. Comparison of conventional Lyot-filter stack with novel Lyot-filter stack using two materials.

This page intentionally left blank.

1. OPTICAL MODEL OF LYOT FILTER

To determine the material property requirements for the WFOV filter, previous Lyot filter designs were reviewed, and the equations relating key filter performance metrics to material properties were determined. The main performance metrics for the filter design include 1) filter resolution, defined as the spectral width transmitted by the filter, 2) free spectral range, defined as the entire spectral bandwidth that is either blocked or transmitted by the filter, and 3) the angular field of view, defined as the incident angular range over which the filter resolution and bandwidth are maintained. The Lyot filter approach has been implemented with a variety of configurations in attempts to improve these metrics, but often very thick crystal plates are required or only modest improvements in performance metrics are achieved. As discussed in the previous section, one promising configuration of the Lyot filter that could offer enhanced performance on all three filter metrics employs a material possessing low birefringence, or even a zero birefringence crossing, but high material birefringence dispersion. If such a material combination exists, the filter could have a large angular field of view and a narrow resolution, which to date has been elusive.

The Lyot filter relies on phase retardation due to birefringence, Γ , which for a single stage is given by the expression [4]:

$$\Gamma = \frac{2\pi}{\lambda} \Delta n d \quad (\text{Equation 1})$$

Here, d is the birefringent plate thickness, and Δn is the difference between the extraordinary and ordinary indices of refraction (i.e. the birefringence). This equation and the following equations in this section were obtained from Reference 4.

The optical transmission, T , through a single stage is given by the expression:

$$T = \frac{1}{2} \left(\cos \frac{\Gamma}{2} \right)^2 \quad (\text{Equation 2})$$

The spectral resolution, $\Delta\lambda_{1/2}$, of the filter is given by:

$$\Delta\lambda_{1/2} = 0.886 * \left| \frac{1}{\frac{2 * d_{thick}}{\lambda} \left(\frac{\partial \Delta n}{\partial \lambda} \frac{\Delta n}{\lambda} \right)} \right| \quad (\text{Equation 3})$$

Here, d_{thick} is the thickness of the thickest stage plate.

The free spectral range, $\Delta\lambda$, of the filter is given by:

$$\Delta\lambda = \left| \frac{1}{\frac{d_{thin}}{\lambda} \left(\frac{\partial \Delta n}{\partial \lambda} \frac{\Delta n}{\lambda} \right)} \right| \text{ (Equation 4)}$$

In this expression, d_{thin} is the thickness of the thinnest stage plate.

The field of view in air, Ω , of the filter is given by:

$$\Omega \approx \pi \theta^2 \approx 0.886 * \pi * n_e * n_o * \left| \frac{\pi}{\Gamma_{thick\ stage}} \right| \text{ (Equation 5)}$$

Here, $\Gamma_{thick\ stage}$ is the phase retardation of the thickest stage of the filter.

As can be observed from these expressions, if a material possesses low or zero birefringence ($\Delta n = 0$) at the operational wavelength, the field of view can be very large, theoretically approaching hemispherical. When this occurs, the spectral resolution and free spectral range are determined solely by the birefringence dispersion, $\Delta n/\Delta\lambda$. With this design principle in place, parametric plots were generated for a variety of spectral resolutions and spectral bandwidths to map out the material birefringence dispersion vs. thickness requirement space. These are shown in Figures 3 and 4.

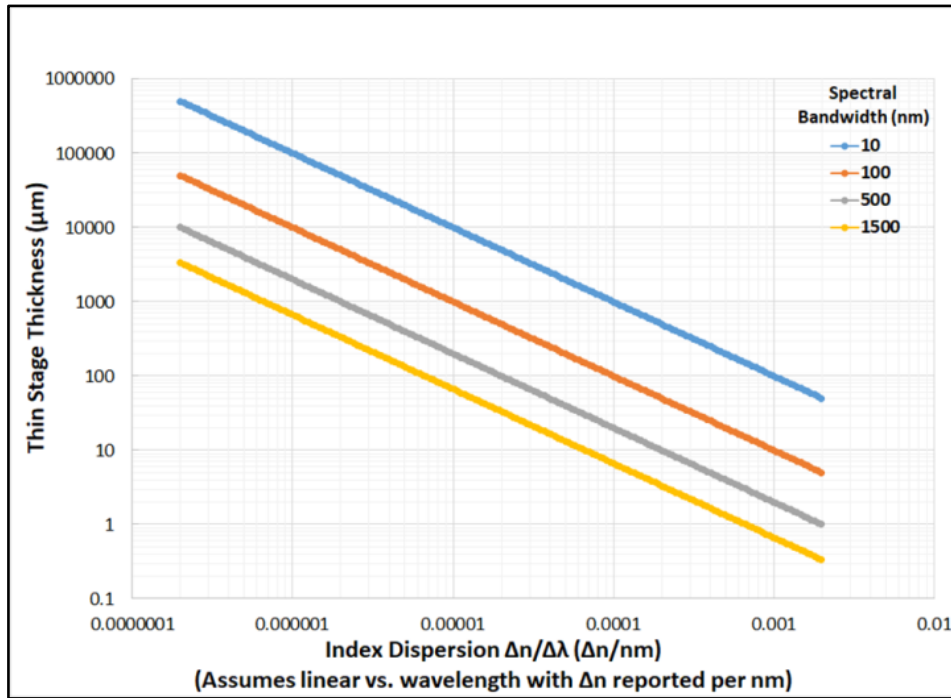


Figure 3. Birefringent plate thickness required for the “thin” stage of a Lyot filter vs. birefringence dispersion for various spectral bandwidths. Zero birefringence at a center operating wavelength of 1000 nm is assumed.

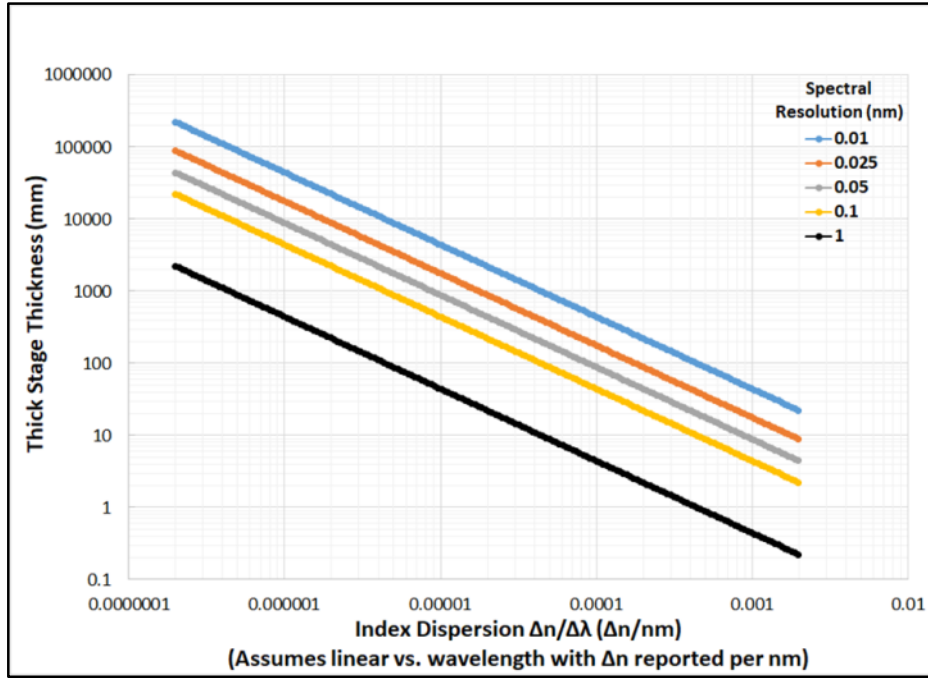


Figure 4. Birefringent plate thickness required for the thickest stage of a Lyot filter vs. birefringence dispersion for various spectral resolutions. Zero birefringence at a center operating wavelength of 1000 nm is assumed.

As can be seen in these figures, the spectral resolution and bandwidth set the plate thicknesses for the thickest and thinnest stages, respectively, with required magnitudes shown for a range of spectral parameters under consideration. These plots then show the required birefringence dispersion a material or material combination must achieve to realize an optical filter with a wide field of view meeting those requirements. It is important to note that this material birefringence dispersion must be met, or exceeded, over the entire spectral bandwidth and simultaneously create a zero birefringence crossing, which was assumed to occur at a wavelength of 1000 nm. From this analysis, it was determined that the material birefringence dispersion is the most critical material metric for assessing potential candidate materials.

Finally, it is worth noting that the number of stages required to meet the spectral resolution and spectral bandwidth requirements of this Lyot filter is determined only by the resolution and bandwidth requirements themselves and not by any particular material properties. The number of stages required is determined by the following expression:

$$\frac{\Delta\lambda}{\Delta\lambda_{1/2}} = \frac{2^N}{0.886} \quad (\text{Equation 6})$$

Here, N is the required number of stages. From this equation, for the target spectral resolution, $\Delta\lambda_{1/2}$, of 0.05 nm and the target wavelength band of 500–1600 nm (which necessitates a free spectral range, $\Delta\lambda$, of 1100 nm), approximately 14 stages are required. If we have 14 stages and require an overall optical transmission >50%, each stage must have a transmission >95%.

This page intentionally left blank.

2. STRATEGY FOR MEETING MATERIAL PROPERTY REQUIREMENTS

As demonstrated above, the magnitude of the birefringence for a candidate material must have a zero crossing at the desired operation wavelength in order to achieve a wide field of view. This attribute can be achieved by combining materials with positive and negative birefringence in a composite structure. To enhance the birefringence dispersion, which was identified as the key material performance metric in the analysis described above, the material composite can be engineered with constituent materials with different dispersions. For most materials, the refractive indices converge as wavelength increases, which will hereafter be referred to as “normal” birefringence dispersion. For some materials, such as GaN, however, the magnitude of the birefringence increases with wavelength over a substantial spectral range, which will be referred to hereafter as “anomalous” birefringence dispersion. The anomalous dispersion of GaN is shown in Figure 5.

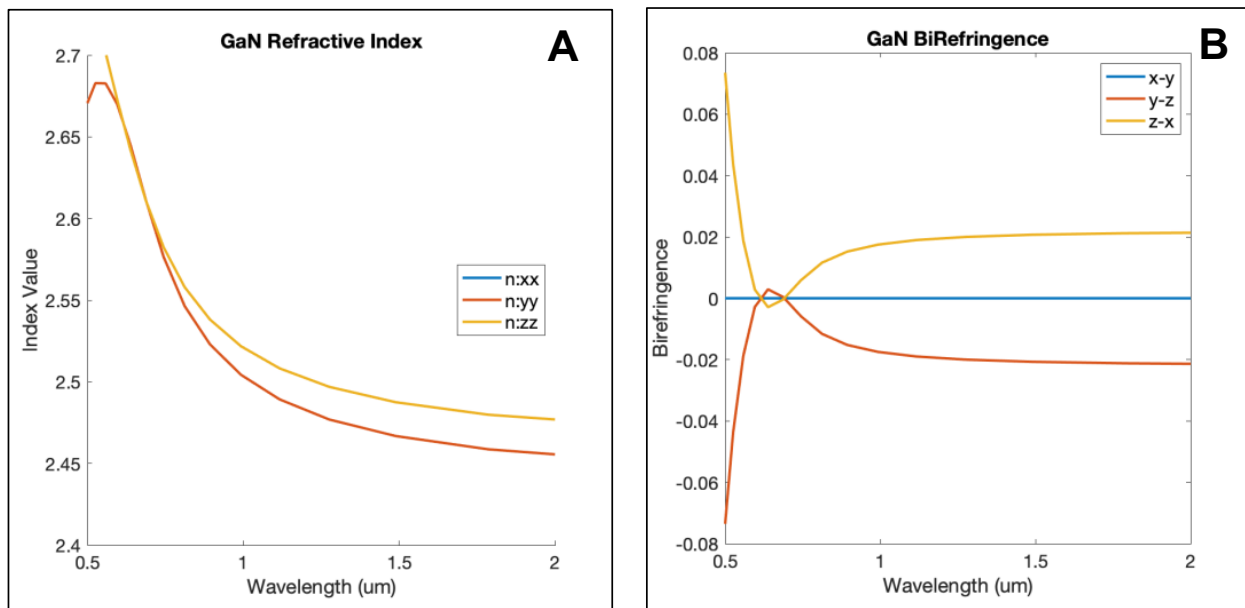


Figure 5. Refractive indices (A) and birefringence (B) for GaN based on Density Functional Theory calculations. GaN exhibits “anomalous” birefringence dispersion, meaning the magnitude of the birefringence increases as a function of wavelength.

3. INITIAL SCREENING OF CANDIDATE MATERIALS

To evaluate the potential of the novel Lyot filter concept described above, a hypothetical filter composed of two of the most common materials with opposite birefringence, GaN and LiNbO₃, was first investigated. These materials, in addition to exhibiting substantial birefringence with opposite signs, are also widely available in the form of large-scale (centimeters or larger) single crystals of high optical quality. This initial material pair was first evaluated with respect to the target filter performance metrics using literature data for optical constants obtained from a database [5]. To determine the overall birefringence dispersion over the target operation wavelength range (500–1600 nm), a Matlab script was created to calculate the overall birefringence of LiNbO₃ and GaN composites with a GaN fraction, x , ranging from 0 to 1 in increments of 0.01. Values of x yielding a zero crossing in the composite birefringence were then determined by the script, and the maximum birefringence magnitude achievable while maintaining a zero crossing was calculated. For the LiNbO₃/GaN material combination, the maximum possible birefringence dispersion (defined as $\Delta n/\text{nm}$) was found to be less than $1 \times 10^{-6} \text{ nm}^{-1}$ (Figure 7). For this dispersion value, achieving even a modest spectral resolution of 1 nm would require a maximum stage thickness of approximately 0.5 m, far beyond the practical thickness range for typical single-crystal specimens.

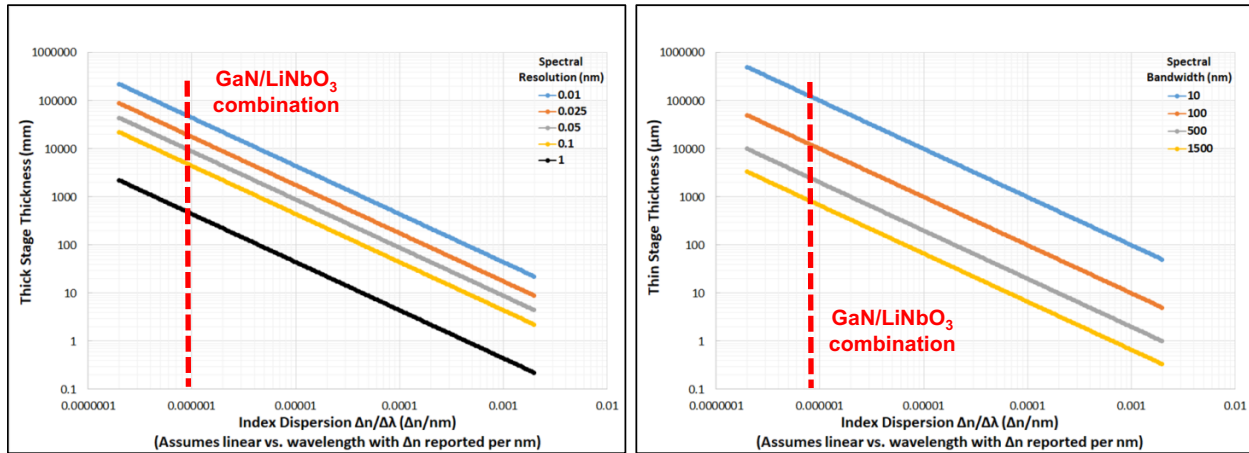


Figure 7. Birefringence dispersion of a LiNbO₃/GaN composite. For the calculated dispersion level, a maximum stage thickness of $>0.5 \text{ m}$ would be required to achieve even a modest 1 nm spectral resolution.

Because of the poor birefringence dispersion of the initially proposed LiNbO₃/GaN composite, alternative candidate materials were surveyed using experimentally measured optical constants obtained from the same database. Data for GaSe were obtained from a previous literature report [6]. Nearly 30 established birefringent materials with experimental data available for both ordinary and extraordinary

polarization and optical bandgaps in excess of 2 eV (to ensure reasonable transparency over 500–1600 nm) were surveyed. The birefringence magnitude (at 1 micron) and the birefringence dispersion were calculated, and the nature of the dispersion, either “normal” (birefringence decreases with increasing wavelength) or “anomalous” (birefringence increases with increasing wavelength) was determined for each material. Results of this survey are shown in Table 2 below.

TABLE 2

Survey of common birefringent materials. The originally proposed materials, LiNbO₃ and GaN, are highlighted in yellow, and the optimum combination of materials from among those surveyed is highlighted in green.

Material	Birefringence Sign	Dispersion Type	Magnitude of $d\Delta n/d\lambda$ (nm⁻¹)	Birefringence Magnitude
CaWO ₄	Positive	Normal	0.0000004	0.0133
Tl ₃ AsSe ₃	Negative	Normal	-1.1E-06	-0.1841
CdGeP ₂	Positive	Anomalous	-4E-07	0.0113
SiO ₂	Negative	Normal	0.0000007	0.0086
Al ₂ O ₃	Negative	Normal	-5E-07	-0.0078
CaMoO ₄	Positive	Normal	0.0000004	0.0058
LiIO ₃	Negative	Normal	-5.5E-06	-0.1313
YLiF ₄	Positive	Normal	0.0000001	0.0220
MgF ₂	Positive	Normal	0.0000006	0.0114
LuAl ₂ (BO ₃) ₄	Negative	Normal	-9.2E-06	-0.0712
CsLiB ₆ O ₁₀	Negative	Normal	-7.8E-06	-0.0463
SiC	Positive	Normal	0.0000018	0.0339
TiO ₂	Positive	Normal	0.0000244	0.2608

TABLE 3 (Continued)

Survey of common birefringent materials. The originally proposed materials, LiNbO₃ and GaN, are highlighted in yellow, and the optimum combination of materials from among those surveyed is highlighted in green.

Material	Birefringence Sign	Dispersion Type	Magnitude of $d\Delta n/d\lambda$ (nm ⁻¹)	Birefringence Magnitude
AgGaS ₂	Negative	Anomalous	0.0000003	-0.0541
YVO ₄	Positive	Normal	0.0000028	0.2040
BaB ₂ O ₄	Negative	Normal	-1.31E-05	-0.1105
LiNbO ₃	Negative	Normal	-7.1E-06	-0.0657
GaN	Negative	Normal	0.0000026	-0.0064
AlN	Positive	Normal	0.0000024	0.0399
CaCO ₃	Negative	Normal	-1.76E-05	-0.1589
GaSe	Positive	Anomalous	0.0002101	0.3426

Combinations of materials with large “normal” and “anomalous” dispersion were analyzed using the Matlab script described above. Using this script, a maximum birefringence dispersion with a zero crossing of 0.000135 nm⁻¹ was obtained for a composite of TiO₂ and GaSe. Results of this analysis are shown in Figure 8 below.

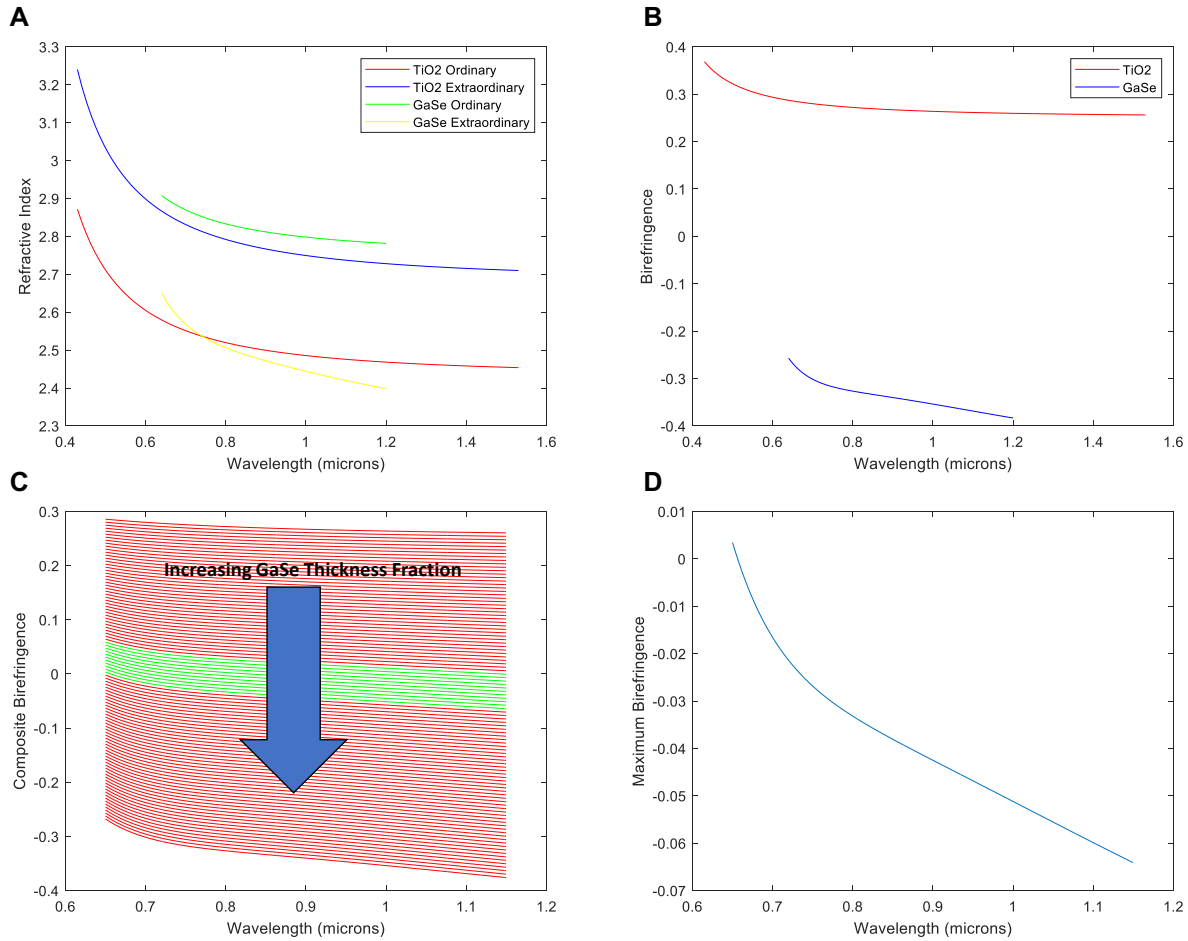


Figure 8. Analysis of the birefringence and birefringence dispersion for a composite of TiO₂ and GaSe. A. Optical constants for TiO₂ and GaSe; B. Birefringence vs. wavelength for TiO₂ and GaSe; C. Composite birefringence vs. wavelength for combinations of TiO₂ and GaSe ranging from pure TiO₂ to pure GaSe; D. Birefringence dispersion for an optimized composite with a zero crossing.

The TiO₂/GaSe composite was found to have an overall birefringence dispersion over two orders of magnitude larger than that for the LiNbO₃/GaN combination, but the required maximum stage thickness to achieve even a modest 1 nm spectral resolution remains of the order of several mm, and a thickness of tens of cm is required to reach the more ambitious 0.05 nm resolution in Table 1 (Figure 9). To improve filter performance at practical stage thicknesses, a broader range of candidate materials must be explored beyond the limited subset of mature optical materials that have been widely characterized experimentally.

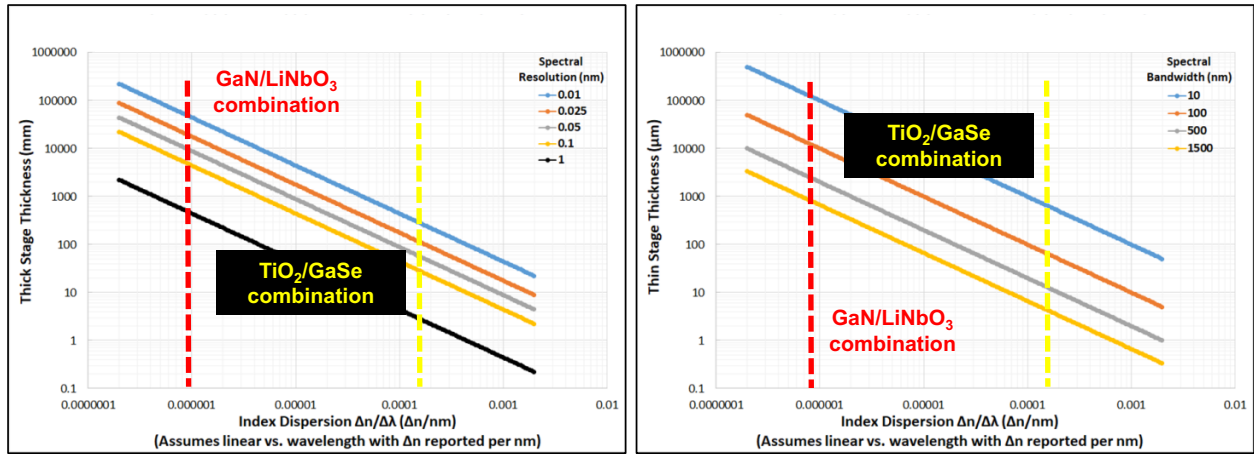


Figure 9. Birefringence dispersion of an optimized TiO_2/GaSe composite. A large improvement can be seen compared to the originally proposed $\text{GaN}/\text{LiNbO}_3$ composite, but the maximum stage thickness remains prohibitive.

This page intentionally left blank.

4. BROADER SCREENING OF CANDIDATE MATERIALS

To search for material candidates with improved birefringence dispersion, a database-mining approach was developed and applied to the Materials Project (MP) database, which contains theoretical calculations of material properties for over 100,000 materials [7]. This database contains information on crystal structure, bandgap, and energy above the convex hull—defined as the stability of a material relative to the most stable state at that composition—for all materials included. This basic information from MP for GaN is shown in Figure 10. Dielectric properties are also calculated for most of these materials; the example for GaN is shown in Figure 11. These properties were the basis for the initial screening process to obtain a list of candidate materials for subsequent first-principles calculations of optical constants using Density Functional Theory (DFT).

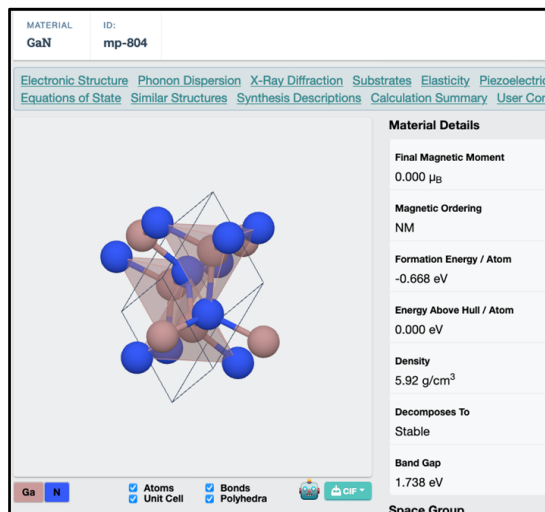


Figure 10. Materials Project entry for GaN showing structure, stability, and bandgap data [7].

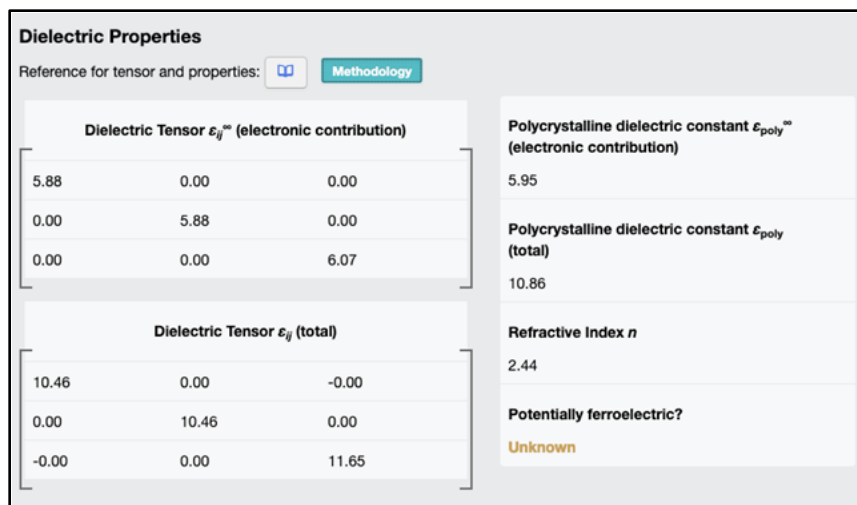


Figure 11. Dielectric properties for GaN from the Materials Project database [7].

The pymatgen python code developed by the Materials Project team was used to extract an initial list of candidate materials [8]. The first parameter used for screening was material stability, determined using energy above the convex hull. It should be noted that the calculated energies in the database are at 0 K. To include materials that would become stable at elevated temperatures and to account for small inaccuracies in the calculated energies, a cutoff of 10 meV/atom above the convex hull was used as a stability criterion.

The second screening parameter was bandgap. Only materials with calculated bandgaps above 2 eV were included in further screening. Although achieving high transparency at wavelengths down to 500 nm requires a bandgap of 2.5 eV, DFT calculations are widely known to underestimate material bandgaps, and thus the bandgap selection criterion was relaxed slightly for initial material screening.

Anisotropy in the optical-frequency dielectric tensors, which is indicative of birefringence, was used as the final screening parameter for generation of the initial candidate list. Application of these screening criteria resulted in a list of 2750 materials. As can be seen in Figure 11, the dielectric properties are not given as functions of wavelength in the MP database, which inhibits direct screening of materials for high birefringence dispersion. However, the magnitude of the birefringence, which is determined by the differences in the diagonal components of the dielectric tensors, is expected to be strongly related to the birefringence dispersion and was thus used as a “proxy” parameter to rank candidate materials. The top 20 candidate materials, ranked by the expected magnitude of the birefringence, are shown in Table 3. This filtered and ordered list served as a guide for detailed screening using DFT calculations.

TABLE 4

Top 20 candidate materials extracted from the Materials Project database ranked by anisotropy in the high-frequency dielectric tensor. Candidate materials have a bandgap greater than 2 eV and are within 10 meV/atom of the convex hull.

Formula	Space Group	Bandgap (eV)	Energy Above Hull (meV/atom)
BrNO ₃	P2 ₁ 2 ₁ 2 ₁	2.57	0
CsBr ₂ F	P4/mmm	2.24	0
HgBr	I4/mmm	2.46	0
Gel ₂	R3m	2.07	1
ScAgP ₂ S ₆	P31c	2.04	0
Sc ₂ C ₃ N ₆	R3c	3.31	0
As ₂ S ₃	P2 ₁ /c	2.20	0
ZrNF	P2 ₁ /c	2.08	0
MgPSe ₃	R3	2.30	0
NaCoO ₂	R3m	2.18	0
GaTeCl	Pnnm	2.17	0
Cd(CN) ₂	R3m	2.34	0
HgCl	I4/mmm	2.82	0
MgAg ₂ P ₂ S ₆	C2/c	2.21	0
BrF ₃	Cmc2 ₁	2.34	0
CdPS ₃	C2/m	2.12	0
KMnIO ₆	P312	2.03	0

TABLE 5 (Continued)

Top 20 candidate materials extracted from the Materials Project database ranked by anisotropy in the high-frequency dielectric tensor. Candidate materials have a bandgap greater than 2 eV and are within 10 meV/atom of the convex hull.

Formula	Space Group	Bandgap (eV)	Energy Above Hull (meV/atom)
In ₂ C ₃ N ₆	R3c	2.15	0
HfBrN	Pmmm	2.13	0
BN	P63/mmc	4.27	0

5. COMPUTATIONAL SCREENING OF CANDIDATE MATERIALS

Ab initio DFT calculations were performed using the Vienna *Ab initio* Simulation Package (VASP) within the projector augmented-wave approach, using the generalized gradient exchange and correlation functional parameterized by Perdew, Burke, and Ernzerhof [9]. For compounds containing O, N, C, or F, energy cutoffs were 500 eV for structural relaxations and 550 eV for dielectric calculations. For all other compounds, energy cutoffs were 300 and 350 eV, respectively. A k-point density of at least 1000 k-points/reciprocal atom was used for all calculations. Ionic and volume relaxations were performed until total energy converged to within 0.1 meV.

Ionic and volume relaxations were performed separately using the blocked-Davidson algorithm [10]. This process was continued until the energy difference between relaxation runs was less than 0.5 meV/atom. The relaxed structure was then utilized in calculations to extract the dielectric tensor and the density of states. These computations were performed using partially self-consistent GW calculations [11]. The number of computed bands was increased by approximately 50% above the number of filled bands. These calculations provided the six components of the frequency-dependent real and imaginary dielectric functions. Wavelength-dependent refractive indices and absorption coefficients were extracted as the real and imaginary components of the square root of the complex dielectric functions.

These calculations were performed for the top 60 materials in the candidate list. The top candidate material, BrNO₃, is a liquid at room temperature (melting point of -42 °C.) and was thus excluded as a candidate material. The third material in the candidate list, HgBr, has similar relevant properties to BrNO₃, but has a melting point above 400 °C. Calculated optical properties for HgBr are shown in Figure 12. The calculated extinction coefficient for HgBr is not ideal, but the large potential birefringence dispersion makes it worthy of experimental validation. Many considerations factor into the decision of which candidate materials should be experimentally validated. This process will be described in the next few sections.

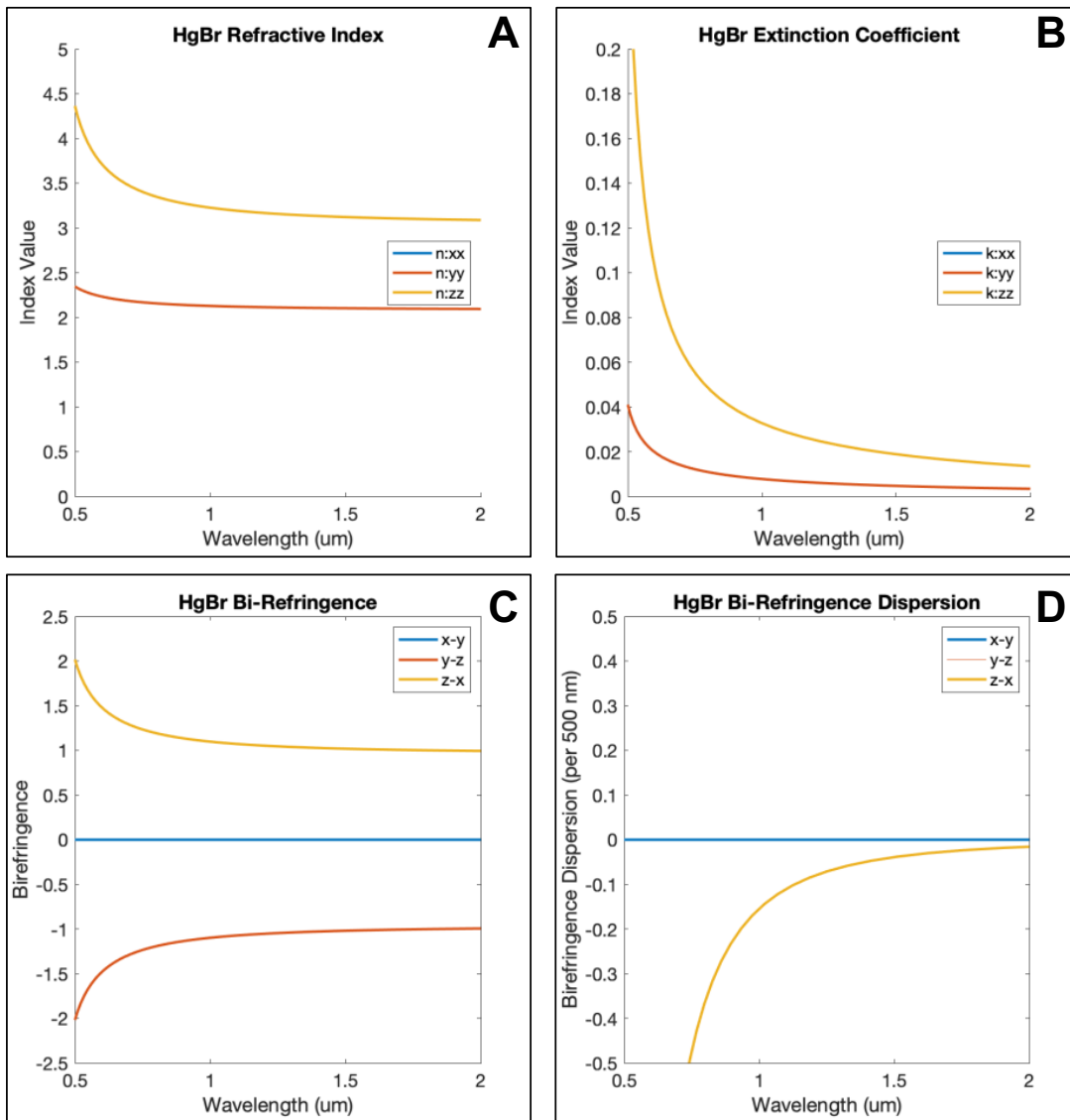


Figure 12. Optical properties for HgBr calculated with DFT, including refractive indices (A), extinction coefficients (B), birefringence (C), and birefringence dispersion (D).

Large variations in dispersion across the wavelength range are common. A number of materials displayed significant dispersion at smaller wavelengths, but weak dispersion in the 1–1.5 micron region. This behavior presents a challenge to the goal of finding a single pair of materials that will work through the entire 500–1600 nm region.

6. EVALUATION OF CANDIDATE MATERIALS FOR LYOT FILTER

Optical constants obtained from DFT calculations were used to calculate material birefringence magnitude and dispersion, as before. As described in previous sections, the maximum possible birefringence while maintaining a zero crossing was calculated using a Matlab script for composites of materials with high “normal” and “anomalous” birefringence dispersions. A combination of HgI (normal dispersion) and GaSe (anomalous dispersion) was determined to have the highest possible composite birefringence dispersion with a zero crossing. The maximum birefringence value was predicted for a composite consisting of 16% HgI and 84% GaSe. Analysis results for the hypothetical HgI/GaSe composite are shown in Figure 13.

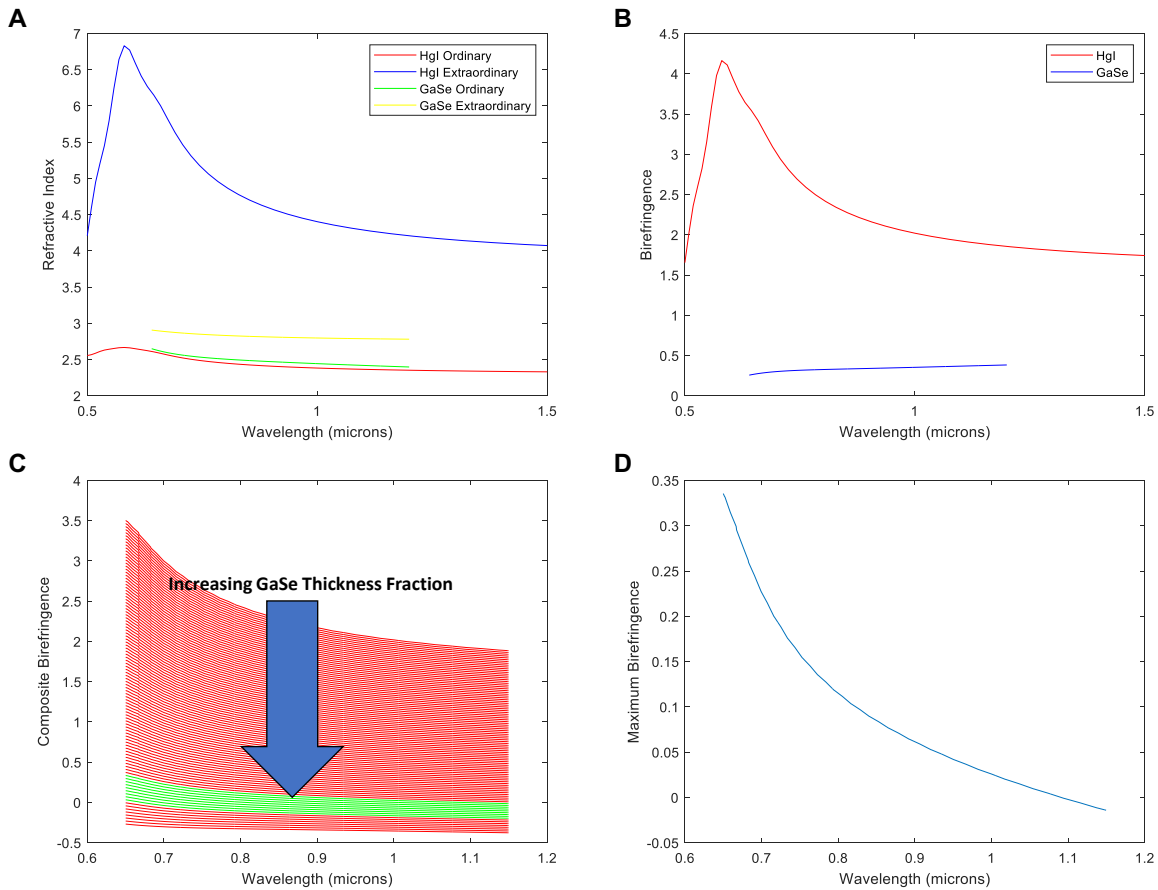


Figure 13. Analysis of the birefringence and birefringence dispersion for a composite of HgI and GaSe. A. Optical constants for HgI and GaSe; B. Birefringence vs. wavelength for HgI and GaSe; C. Composite birefringence vs. wavelength for combinations of HgI and GaSe ranging from pure HgI to pure GaSe; D. Birefringence dispersion for an optimized composite with a zero crossing.

A maximum birefringence of 0.0007 was calculated for the optimized HgI/GaSe composite. This value, if validated experimentally, would represent an improvement of nearly three orders of magnitude over the initially proposed LiNbO₃/GaN composite, demonstrating the power of the materials-by-design methodology for identifying new materials that are not intuitively obvious. As shown in Figure 14, the target spectral resolution of 0.05 nm listed in Table 1 can be achieved for a maximum stage thickness of ~1 cm—within the size range of typical single-crystal specimens. These results, thus, suggest a viable pathway to a Lyot filter with a wide field of view, a high spectral resolution, and a wide bandwidth.

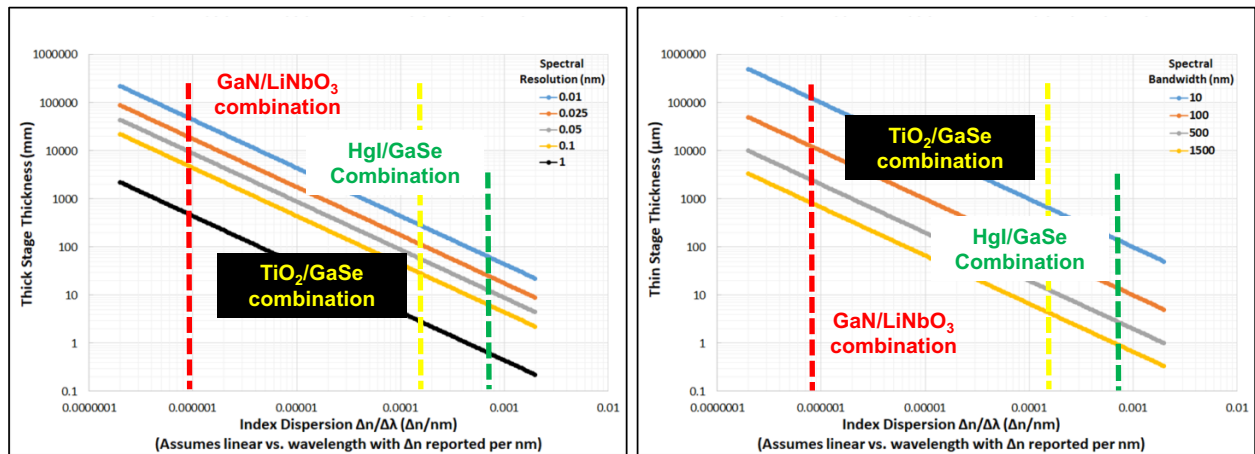


Figure 14. Birefringence dispersion of optimized HgI/GaSe composite. A large improvement can be seen compared to the originally proposed GaN/ LiNbO₃ composite, and reasonable filter performance parameters can be achieved for experimentally feasible maximum stage thickness values.

Further improvement in the composite birefringence dispersion is impeded by the dearth of materials with “anomalous” dispersion. Broad screening of candidate materials using database mining and first-principles theory calculations revealed several materials with “normal” dispersion values greater than those for established birefringent materials, but few materials with large, anomalous dispersion were identified. Detailed analysis of the candidate materials, however, revealed that anomalous dispersion occurs frequently in materials with particular generic chemical formulas and specific space groups. As shown in Table 4, IV-VII₂ materials with the Pnma space group, compounds with the generic formula ABC₂ and the I-42d space group, binary semiconductors with the P63mc space group (wurtzite structure), and binary semiconductors with the R3m space group were found to have anomalous dispersion frequently. Machine-learning algorithms developed by the MIT Lincoln Laboratory Artificial Intelligence Technology Group may reveal further connections linking material stoichiometry, constituent elements, and crystal structure to anomalous birefringence dispersion; such linkages could prove invaluable for identifying and optimizing a material with large, anomalous dispersion.

TABLE 6

Comparison of materials with anomalous birefringence dispersion. Anomalous dispersion appears to be common for particular material families, defined by a generic chemical formula and space group [5], [6].

Material	Space Group	Experiment or Theory?
PbBr ₂	Pnma	Experiment
PbCl ₂	Pnma	Experiment
CdGeP ₂	I-42d	Experiment
AgGaS ₂	I-42d	Experiment
CuGaSe ₂	I-42d	Both
CdS	P63mc	Experiment
GaN	P63mc	Both
GaSe	R3m	Both
GaS	R3m	Both

To determine the ability of first-principles calculations of optical constants to identify anomalous dispersion, optical constants derived from experimental databases were compared with optical constants calculated by DFT for several materials, including GaS, GaSe, and CuGaS₂, for which anomalous dispersion within the range of interest (500–1500 nm) has been shown experimentally. For all materials examined, anomalous dispersion was observed over at least several hundred nm of the target spectral range in DFT calculations. A comparison of experimental [6] and theoretical optical constants for GaSe, the top candidate material with anomalous dispersion, demonstrates reasonable agreement and anomalous dispersion over the range of 0.6–0.9 microns, as shown in Figure 15. The results of this study suggest that DFT calculations can enable successful identification of candidate materials with anomalous dispersion.

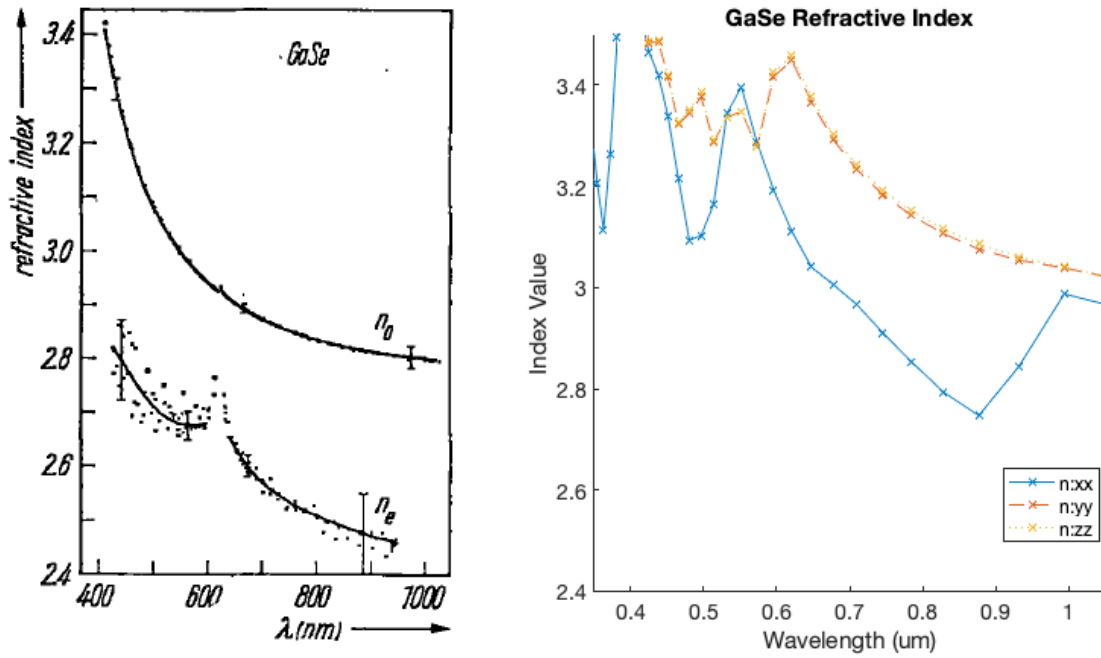


Figure 15. Comparison of experimental (left) and calculated (right) optical constants for GaSe. Anomalous birefringence dispersion can be observed in both theory and experiment over the range of 0.6–0.9 microns [6].

7. SELECTION OF MATERIALS FOR EXPERIMENTAL SYNTHESIS

Top candidate materials identified through database mining and first-principles theory were further analyzed for the feasibility of synthesizing single-crystal specimens. For the top candidate materials with high birefringence dispersion listed in Table 5, literature procedures for synthesis of bulk single crystals were sought and, where available, analyzed for feasibility. Due to the lack of available equipment at MIT LL for Bridgman, Czochralski, and other common single-crystal growth methods, materials that can be synthesized readily using low-cost equipment were prioritized. Several top candidate materials have established literature protocols for synthesis of single crystals using simple and low-cost methods, such as precipitation from a solvent (flux crystallization) or heating of constituent elements in sealed ampoules. From this analysis, HgBr, AsI₃, and Cd(CN)₂ were identified as the first material candidates for synthesis trials. In addition, commercial sources were identified for single crystals of four other materials, GaSe, Sb₂S₃, MoO₃, and SbSI. These seven materials will be the first to be analyzed experimentally.

TABLE 7

Comparison and prioritization of top candidate materials for experimental validation.

Material	Max. Biref. Dispersion	Solvents	Literature Procedures for Crystal Growth	Procedures for Flux Growth	Available Commercially	Comments	Overall Priority
AsI ₃	0.000162	CS ₂	Yes	Yes	No		
BiTeCl	0.00036	Unknown	Yes	No	No	Ampoule synthesis possible	
Cd(CN) ₂	0.001171	Water	Yes	Yes	No		
CsBr ₂ F	0.000321	Unknown—water?	Yes	No	No	Ampoule synthesis possible	
GaSe--R3m	0.000387	Bi	Yes	Yes	Yes		
GaTeCl	0.000309	Unknown	Yes	No	No	Ampoule synthesis possible	

TABLE 8 (Continued)

Comparison and prioritization of top candidate materials for experimental validation.

Material	Max. Biref. Dispersion	Solvents	Literature Procedures for Crystal Growth	Procedures for Flux Growth	Available Commercially	Comments	Overall Priority
HgBr	0.000358	Possibly ammonia	No	No	No		
HgI	0.001476	Possibly ammonia	No	No	No	Can't identify source for HgI	
K ₂ PtC ₂	0.000695	Unknown	No	No	No	Literature for polycrystals	
KMnIO ₆	0.001562	Unknown	Yes	No	No	Synthesis may be adapted for flux growth	
MoO ₃	0.00049	Water	Yes	Unknown	Yes		
NaCoO ₂	0.00074	Unknown	Yes	No	No		
NaMnO ₂	0.001782	Unknown	Yes	No	No		
RbNdO ₂	0.001577	Unknown	No	No	No		
RbNdS ₂	0.000259	Unknown	No	No	No		
Sb ₂ S ₃	0.000661	Acids?	Yes	Possible	Yes		
SbSBr	0.000206	SbI ₃ , water?	Yes	Yes	No	Gel growth process in solution	
SbSI	0.000506	SbI ₃ , water?	Yes	Yes	Yes		

 Initial materials for experimental validation

8. DESIGN AND CONSTRUCTION OF CRYSTAL GROWTH APPARATUS

To enable growth of single-crystal specimens of candidate materials using flux crystallization, a versatile and low-cost method, a flux crystallization apparatus was designed and constructed at MIT LL. This apparatus, shown in Figure 16, consists of three parallel crystallization reactors. Nitrogen gas can be introduced at a controlled rate via mass flow controllers, enabling controlled evaporation of a solvent, and the crystallization vessels can be slowly cooled over a period of several days, enabling precipitation of single crystals from a supersaturated solution. Evaporated solvent from the crystallization vessels is collected downstream in jacketed flasks for disposal. This apparatus enables a maximum temperature of 400 °C in the reaction flasks and supports precise temperature control using thermocouple probes and a three-channel PID temperature controller.

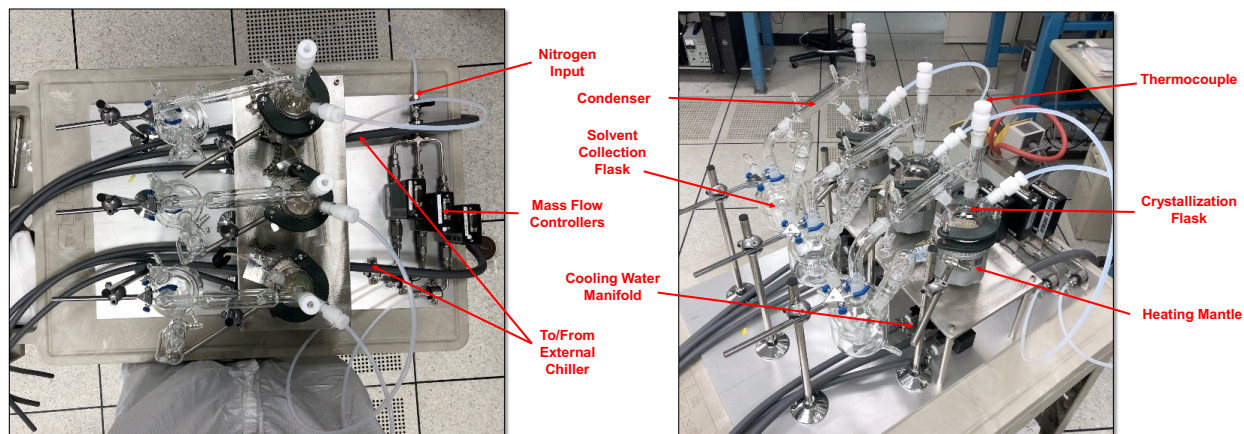


Figure 16. Apparatus for growth of single crystals using precipitation from solution. Crystals can be grown either by slow, controlled evaporation of solvent or by slow cooling of a saturated solution.

This page intentionally left blank.

SUMMARY AND CONCLUSIONS

A novel concept for a birefringent Lyot filter has been proposed that employs a pair of materials with opposite birefringence magnitude and dispersion. An analytical model for Lyot filters indicates that the proposed concept can simultaneously achieve high spectral resolution, high free spectral range, and a wide field of view for a combination of materials with a low birefringence magnitude and a large birefringence dispersion. For a given birefringence dispersion, filter performance is limited by the thickness of the thickest wave plates, which is constrained by the size of single crystals that can be grown practically (typically of the order of a few centimeters). Filter modeling further indicates that birefringence dispersion can be enhanced by combining materials with “normal” birefringence dispersion (birefringence decreases with wavelength) and “anomalous” birefringence dispersion (birefringence increases with wavelength). Thousands of candidate materials were screened for birefringence dispersion using a combination of automated database mining from the Materials Project database and Density Functional Theory calculations. The top candidate material pair, HgI and GaSe, yields a birefringence dispersion of $7 \times 10^{-4} \text{ nm}^{-1}$, which is sufficient to achieve the target spectral resolution of 0.05 nm for a maximum waveplate thickness of approximately 1 cm. This thickness value is within the size range of single crystals that are routinely synthesized, indicating that experimental realization of the proposed novel Lyot filter may be feasible. To facilitate fabrication of a prototype filter, an apparatus for flux crystallization and experimental validation of top candidate materials was designed and constructed. Successful realization of the proposed filter is expected to enable new applications in astronomical imaging, spectral filtering for tunable laser sources, and many other critical areas.

This page intentionally left blank.

REFERENCES

- [1] B. Lyot, "Optical apparatus with wide field using interference of polarized light," *Acad. Sci.* **197**, 1593 (1933).
- [2] S. Saeed and P. J. Bos, "Multispectrum, spatially addressable polarization interference filter," *J. Opt. Soc. Am. A* **19**, 2301 (2002).
- [3] C. Trefzger and J. Solf, "Calibration of spectrograms using a Lyot filter element," *Astron. Astrophys.* **63**, 131 (1978).
- [4] P. Yeh, "Dispersive birefringent filters," *Opt. Commun.* **37**, 153 (1981).
- [5] M. N. Polyanskiy, "Refractive index database," <https://refractiveindex.info>. Accessed 2021-12-09.
- [6] T. A. McMath and J. C. Irwin, "Indices of refraction of GaS and GaSe," *Phys. Stat. Sol. A* **38**, 731 (1976).
- [7] A. Jain, et al., "The Materials Project: A materials genome approach to accelerating materials innovation," *APL Mater.* **1**, 011002 (2013).
- [8] S. P. Ong, et al., "Python materials genomics (pymatgen): A robust, open-source Python library for materials analysis," *Comput. Mater. Sci.* **68**, 314 (2013).
- [9] G. Kresse and J. Furthmüller, "Efficient iterative schemes for ab initio total-energy calculations using a plane-wave basis set," *Phys. Rev. B* **54**, 11169 (1996).
- [10] E. R. Davidson, "The iterative calculation of a few of the lowest eigenvalues and corresponding eigenvectors of large real-symmetric matrices," *J. Comput. Phys.* **17**, 87 (1975).
- [11] M. Shishkin and G. Kresse, "Self-consistent *GW* calculations for semiconductors and insulators," *Phys. Rev. B* **75**, 235102 (2007).

This page intentionally left blank.

REPORT DOCUMENTATION PAGE			<i>Form Approved</i> OMB No. 0704-0188		
Public reporting burden for this collection of information is estimated to average 1 hour per response, including the time for reviewing instructions, searching existing data sources, gathering and maintaining the data needed, and completing and reviewing this collection of information. Send comments regarding this burden estimate or any other aspect of this collection of information, including suggestions for reducing this burden to Department of Defense, Washington Headquarters Services, Directorate for Information Operations and Reports (0704-0188), 1215 Jefferson Davis Highway, Suite 1204, Arlington, VA 22202-4302. Respondents should be aware that notwithstanding any other provision of law, no person shall be subject to any penalty for failing to comply with a collection of information if it does not display a currently valid OMB control number. PLEASE DO NOT RETURN YOUR FORM TO THE ABOVE ADDRESS.					
1. REPORT DATE (DD-MM-YYYY) 03/03/2022	2. REPORT TYPE Project Report (Line Supported Program)		3. DATES COVERED (From - To)		
4. TITLE AND SUBTITLE Wide-Field-of-View Lyot Filter: FY21 Line-Supported Optical Systems Program			5a. CONTRACT NUMBER		
			5b. GRANT NUMBER		
			5c. PROGRAM ELEMENT NUMBER		
6. AUTHOR(S) M.J. Polking, W.D. Herzog, S. Kaushik, S.M. Redmond, K.J. Tibbets, C.A. Primmerman			5d. PROJECT NUMBER 2238-44 (WBS)		
			5e. TASK NUMBER		
			5f. WORK UNIT NUMBER		
7. PERFORMING ORGANIZATION NAME(S) AND ADDRESS(ES) MIT Lincoln Laboratory 244 Wood Street Lexington, MA 02421-6426			8. PERFORMING ORGANIZATION REPORT NUMBER LSP-355		
9. SPONSORING / MONITORING AGENCY NAME(S) AND ADDRESS(ES) The Lincoln Laboratory Optical Systems Technology Line and Under Secretary of Defense for Research and Engineering Department of Defense			10. SPONSOR/MONITOR'S ACRONYM(S) USD(R&E)		
			11. SPONSOR/MONITOR'S REPORT NUMBER(S)		
12. DISTRIBUTION / AVAILABILITY STATEMENT Distribution A					
13. SUPPLEMENTARY NOTES					
13. ABSTRACT Lyot filters employ differential phase retardation for orthogonal polarizations of light induced by stacks of birefringent waveplates. Lyot filters are widely used for filtering the emission spectra of tunable lasers and for astronomical imaging, particularly for solar observation. Achieving filters with simultaneously high spectral resolution, free spectral range, and field of view, however, remains an outstanding challenge. In this paper, a novel concept for a Lyot filter is described that employs a combination of two materials with opposing signs for both birefringence magnitude and dispersion. An analytical model of this design indicates that a large field of view can be achieved while maintaining high spectral resolution and free spectral range for material combinations that yield a zero-crossing of the birefringence magnitude but a large birefringence dispersion. Candidate material combinations for the novel filter design are surveyed, first with experimental data for common birefringent materials, and subsequently with automated database mining algorithms and first-principles materials theory.					
15. SUBJECT TERMS					
16. SECURITY CLASSIFICATION OF:			17. LIMITATION OF ABSTRACT None	18. NUMBER OF PAGES 49	
a. REPORT UNCLASSIFIED	b. ABSTRACT UNCLASSIFIED	c. THIS PAGE UNCLASSIFIED			19a. NAME OF RESPONSIBLE PERSON
			19b. TELEPHONE NUMBER (include area code)		

